Available online at www.sciencedirect.com
ScienceDirect
Geochimica et Cosmochimica Acta 71 (2007) 615–623
Geochimica
www.elsevier.com/locate/gca

Enthalpy of water adsorption and surface enthalpy of lepidocrocite (γ-FeOOH)

Juraj Majzlan [a,*], Lena Mazeina [b], Alexandra Navrotsky [b]

[a] Institute of Mineralogy and Geochemistry, Alberstraße 23b, Albert-Ludwig University, D-79104 Freiburg, Germany
[b] Thermochemistry Facility, One Shields Ave, University of California at Davis, Davis, CA 95616, USA

Received 29 June 2006; accepted in revised form 16 October 2006

Abstract

Lepidocrocite (γ-FeOOH) appears to be thermodynamically metastable with respect to goethite (α-FeOOH) and yet the former phase forms and persists both in nature and laboratory. Here we show that the thermodynamic factors relevant to these observations cannot be dismissed, although kinetics undoubtedly plays a significant role in the formation and preservation of metastable phases. To understand the relationships of the FeOOH polymorphs in the bulk and nanoscale, we investigated the energetics of lepidocrocite nanoparticles. We measured enthalpy of water adsorption and enthalpy of formation of lepidocrocite samples with surface area of 42–103 m^2/g. Having both quantities measured allowed us to calculate the surface enthalpy for a water-free surface of this phase as 0.62 ± 0.14 J/m^2 and the energy of a relaxed (hydrated) surface as 0.40 ± 0.16 J/m^2. Our measurements show that a portion of the adsorbed water (~40% under laboratory conditions) is chemisorbed (strongly bound) with enthalpy of adsorption of -65.8 ± 2.6 kJ/mol of H_2O relative to vapor (or -21.8 ± 2.6 kJ/mol relative to liquid water). The standard enthalpy of formation from elements for a hypothetical lepidocrocite with nominal composition FeOOH and zero surface area is -552.0 ± 1.6 kJ/mol. Our results demonstrate that when considering the thermodynamic properties of iron oxides in the environment, a conclusive statement about their stability cannot be made without specifying the particle size of individual phases.

1. Introduction

Lepidocrocite (γ-FeOOH) is an orange, fine-grained mineral confined in its occurrences to surficial terrestrial environments. Despite the fact that this phase is metastable with respect to goethite (α-FeOOH) (Majzlan et al., 2003), it can be prepared in the laboratory and is known from nature. Lepidocrocite has been described from soils (Fitzpatrick et al., 1985; Dos Anjos et al., 1995), deep sea sediments (Goldman et al., 2002), and assumed to exist on Mars (Posey-Dowty et al., 1986). Laboratory experiments have shown that lepidocrocite forms easily by a relatively rapid oxidation of aqueous Fe(II) and subsequent hydrolysis of Fe(III) (Posey-Dowty et al., 1986; Schwertmann and Fechter, 1994; Barton et al., 1990; Carlson and Schwertmann, 1990). The formation of lepidocrocite can be enhanced or suppressed by variation of the type of counterion in the solution, pH, rate of oxidation, or the type of oxidation medium.

As a metastable phase, lepidocrocite persists at pedogenic time scales (thousands of years, Schwertmann and Cornell, 2000). Recent investigations in polymorphic systems whose phases tend to form very small particles (e.g., Ranade et al., 2002; Pitcher et al., 2005) have shown that the persistance of the metastable polymorph may not be solely due kinetic factors. If very fine particles are formed, the energy stored in their surfaces and interfaces becomes a significant contribution to the overall energy of the phase (Navrotsky, 2004). The surface energy of the polymorphs has to be taken into account because it may alter the stability relationships of the polymorphs. Often, the polymorph that is metastable in its "bulk" state may become stable in the nano scale (Ranade et al., 2002; Navrotsky, 2004; Pitcher et al., 2005) because it has a lower surface energy.

* Corresponding author. Fax: +49 761 203 6407.
E-mail address: Juraj.Majzlan@minpet.uni-freiburg.de (J. Majzlan).

0016-7037/$ - see front matter © 2006 Elsevier Inc. All rights reserved.
doi:10.1016/j.gca.2006.10.010

Because the system FeOOH shows extensive polymorphism (goethite, lepidocrocite, akaganeite, feroxyhyte), and all these phases tend to form submicron to nanometer sized particles, we are measuring their bulk and surface thermodynamic properties (Majzlan et al., 2003; Mazeina and Navrotsky, 2005; Mazeina et al., 2006). In this contribution, we report the surface thermodynamic properties of lepidocrocite. We measured enthalpy of water adsorption and enthalpy of formation of lepidocrocite samples with several different surface areas. Having both quantities measured allowed us to calculate the surface enthalpy for a dry, water-free surface, as well as for a relaxed hydrated surface of lepidocrocite.

2. Materials and methods

2.1. Materials

The samples LP42, LP77, and LP90 were synthesized by rapid oxidation of a ferrous chloride solution (Schwertmann and Cornell, 2000). The solution (300 ml distilled water + 8.95 g $FeCl_2 \cdot 4H_2O$) was filtered immediately after preparation to remove traces of akaganeite formed by oxidation of the ferrous chloride. The filtrate was then brought to the desired pH (5.5 or 6.0, see below) with 1 N NH_4OH with stirring. Dark-green, voluminous precipitate formed immediately. Afterwards, the oxygen supply was opened and the flow rate adjusted to ~40 ml/min. Oxidation of Fe^{2+} and hydrolysis of Fe^{3+} caused continuous pH drop which was compensated throughout the synthesis by dropwise addition of 1 N NH_4OH. The reaction was complete when pH stabilized without a further addition of hydroxide; the suspension was bright orange with no traces of greenish tinge. The sample LP77 was prepared at pH 5.5. The sample LP90 was prepared at pH 5.5, with 75 mg of K_2HPO_4 added to the solution after filtration (Naono and Nakai, 1989). The sample LP42 was prepared at pH 6.0 with addition of 10.52 g NaCl after filtration (Taylor, 1984). The samples were then washed several times, dialyzed for 3 weeks, and dried at 40 °C.

The sample LP103 was synthesized by titrating 500 ml of 0.1 M $FeCl_2$ and 0.6 M NH_4Cl by 1 M NH_4OH (Sudakar et al., 2003). During the titration, oxygen was constantly bubbled through the solution at a rate of 10 ml/min and pH was maintained at 5.5–6.0 by adding NH_4OH. After the bright yellow sediment formed and pH stabilized for ~1 h, 50 ml of ethanol was added to prevent particles from agglomeration. After keeping the sediment in the mother solution for several hours, the solution was decanted, the solid sample dialyzed for 2 weeks with a water change 3–4 times a day and freeze-dried.

2.2. Characterization

X-ray diffraction (XRD) patterns of the samples were collected with a Scintag PAD V diffractometer using Cu Kα radiation and a diffracted-beam graphite monochromator. The XRD patterns were collected after the synthesis, after degassing (sample surface thoroughly dehydrated), and after soaking of the sample for 2 days in excess water. In the latter case, a wet paste was used for the XRD scan. The patterns were collected from 10° to 70° 2θ with a step size of 0.02° 2θ and dwell time of 15 s. Lattice parameters of the samples were derived by a Rietveld refinement using the program GSAS (Larson and von Dreele, 1994).

Fourier-transform infrared (FTIR) spectra of synthesized samples and samples after degassing at 150 °C were collected with a Bruker Equinox 55 spectrometer using the KBr pellet technique. The FTIR spectra were recorded immediately after pellet preparation. The spectrometer was flushed continuously with nitrogen to minimize contamination by atmospheric water and CO_2 during analysis. Spectra were collected in the 400–4000 cm^{-1} range with a resolution of 4 cm^{-1}. A baseline correction was applied.

The total water content was determined from weight loss upon ignition in air at 1100 °C for 12 h in corundum crucibles. The excess water content was calculated as a difference between the total water content and the stoichiometric water content of FeOOH (10.14 wt%). Before the experiment, the corundum crucibles were annealed at 1100 °C. The total water content of the samples was constant throughout the duration of the experiments because the temperature and relative humidity are always maintained at 22–25 °C and 43–53%, respectively, in our laboratory.

Surface area was measured by the BET (Brunauer–Emmett–Teller) (Brunauer et al., 1938) method with a Micromeritics ASAP 2020 apparatus. The samples were vacuum (<0.5 Pa) degassed at 150 °C for at least 12 h. Measurements were performed in a liquid nitrogen bath with N_2 as the adsorbate gas. Five data points in the range of 0.05–0.30 P/P_0 were collected for each sample. Surface area was calculated using the cross-sectional area of $N_2 = 16.2$ Å^2.

2.3. Calorimetric measurements

Acid-solution calorimetry was carried out with a Hart Scientific IMC-4400 isothermal calorimeter. The enthalpy of solution (ΔH_{sol}) was measured by dissolving approximately 5 or 10 mg of a pelletized sample in 25.0 ml of 5.0 N HCl (Alfa Aesar), maintained at 25.00 ± 0.01 °C. The measured heat effect was 5–6 J. In a separate set of experiments, we determined that the calorimeter in this configuration is capable of detecting effects of 0.02 J. Calorimeter calibration was performed by dissolving KCl (NIST standard reference material 1655) in deionized water at the same temperature.

The initial state in every calorimetric experiment is a crystalline lepidocrocite sample and 5 N HCl. The final state is a dilute solution of Fe^{III} in 5 N HCl. At such a high concentration of HCl, the predominant Fe^{III} species are $FeCl_2^+$ complexes (Tagirov et al., 2000). Since iron concentration in the acidic solution is very similar for the samples

(LP77, LP90, LP103) and the reference phase (LP42), all $FeCl_2^+$ complexes cancel out in the thermochemical cycles. For this reason, these aqueous species will not be considered further in the thermochemical cycle in this paper.

Water adsorption calorimetry was carried out by a home-built combination of two commercial instruments, a Micromeritics ASAP 2000 analyzer and a SETARAM DSC111 Calvet-type microcalorimeter (Ushakov and Navrotsky, 2005) operated at 25 °C. The technique combines precision gas dosing and volumetric detection of amount of adsorbed gas with an accurate measurement of the heat exchanged in the adsorption process. The calorimeter was calibrated by measurements of the enthalpy of Ga fusion and heat carried by laser pulses of known pulse duration (180 s) and power (3.2 mW). Both calibration factors are in agreement within the experimental error, thus confirming their reliability. Prior to the water adsorption experiment, the samples were degassed at 150 °C for at least 12 h to remove as much water from the surface of lepidocrocite as possible. Remaining water was determined from the weight loss of the sample during degassing (by subtracting from the total excess water content) and additionally by firing the sample at 1100 °C as described above. After degassing, the BET surface area was measured. Preliminary to adsorption experiments, samples were evacuated again for several hours at room temperature. The criterion of sufficient sample degassing was a sample leak rate of <13.3 mPa/s. After the system stabilized, water vapor was introduced in a series of small dosing steps. The heat of adsorption of each dose was recorded by the calorimeter. The measured heat effects after each dose of water vapor were in the range of 20–180 mJ. Thus, a simultaneous record of the equilibrium relative pressure after each vapor dose and the adsorption enthalpy was obtained.

The *differential enthalpy* of adsorption ($\Delta H_i^{\mathrm{dif}}$) is calculated as

$$\Delta H_i^{\mathrm{dif}} = \frac{Q_i}{w_i \cdot m \cdot 4.46 \cdot 10^{-5}} \tag{1}$$

where Q_i is the measured heat effect, w_i is the amount of adsorbed water (in cm^3/g of sample), m is the sample mass, and the factor 4.46×10^{-5} (in mol/cm^3) corresponds to the amount of the gas vapor in 1 cm^3 at STP.

Integral enthalpy at a given coverage j is the sum of the heats Q_i divided by the total amount of adsorbed water up to the given coverage j

$$\Delta H_j^{\mathrm{int}} = \sum_1^j Q_i / \sum_1^j w_i \cdot m \cdot 4.46 \cdot 10^{-5} \tag{2}$$

A correction corresponding to water adsorbed on the walls of the sample holder was applied for all samples. For this purpose, water adsorption was performed as described above with the empty quartz sample holder. Total amount of adsorbed water (for both sample and sample holder) at each step was integrated as follows:

$$S_j = \sum_1^j (P_i - P_{i-1}) \cdot V_i = (P_i - P_{i-1}) \cdot V_i + S_{j-1} \tag{3}$$

where P_i stands for the relative pressure P/P_0 at each step and V_i is the volume of water adsorbed at each step in cm^3. S_j for the water adsorbed on the walls was then plotted as a function of P_i and fitted by a sixth order polynomial. This polynomial was then used to calculate the amount of water adsorbed on the sample holder walls, S_i^{wall}, at the given P_i of the particular sample. This amount was then subtracted from the amount of water adsorbed on the sample.

$$S_i^{\mathrm{corr}} = S_i^{\mathrm{sample}} - S_i^{\mathrm{wall}} \tag{4}$$

Corrected w_i^{corr} doses were then recalculated from the corrected amount of water using the following formula:

$$w_i^{\mathrm{corr}} = \frac{(S_i^{\mathrm{corr}} - S_{i-1}^{\mathrm{corr}})}{(P_i - P_{i-1}) \cdot m} \tag{5}$$

Corrected integral enthalpy would be accordingly

$$\Delta H_j^{\mathrm{int}}(\mathrm{corr}) = \sum_1^j Q_i / \sum_1^j w_i^{\mathrm{corr}} \cdot m \cdot 4.46 \cdot 10^{-5} \tag{6}$$

Calorimetric signal of water adsorption on the walls of the quartz sample holder was negligible and did not need any corrections.

3. Results

XRD patterns of all samples could be indexed in the orthorhombic cell of lepidocrocite and the calculated lattice parameters (Table 1) agree well with those published previously for this phase (Zhukhlistov, 2001). No peaks of other phases were detected. The difference in the lattice parameter b (equal to the interlayer distance) between the samples after degassing and the same samples after soaking in water for 2 days was 0.02–0.04 Å.

The FTIR bands correspond to those assigned to lepidocrocite (Lewis and Farmer, 1986). No carbonate or CO_2 bands could be discerned in the collected spectra, suggesting that only H_2O was desorbed. This finding is important because other iron oxides, such as goethite, have high affinity for CO_2 and may include carbonate groups in their structure (Boily et al., 2006). Results of the loss on ignition experiments and the water content as moles of excess water per mole of FeOOH are shown in Table 1.

For an accurate measurement of the energetics of water adsorption, it is critical to dehydrate the surface of the material as much as possible. Our tests have shown that lepidocrocite looses all adsorbed water after 12 h treatment at 150 °C. The excess water content (water content greater than that of the FeOOH stoichiometry), measured after the degassing procedure, was equal to zero within the uncertainty for all samples. No phase transformation was detected by XRD and FTIR after this treatment. The experiments were performed until the relative pressure of water vapor reached the value of $P/P_0 \sim 0.3$–0.5 (Fig. 1).

Table 1
Crystallite size, surface area, water content as moles of excess water per mole of formula unit ($FeOOH \cdot xH_2O$), and lattice parameters of the studied samples

Sample	Excess water		BET surface area (m^2/g)	Lattice parameters		
	x (mol)	Coverage θ (H_2O/nm^2)		a (Å)	b (Å)	c (Å)
LP103	0.24[a] ± 0.02[b] (6)[c]	15.8	103.3 ± 0.4	3.0671 (7)	12.521 (5)	3.8701 (9)
LP90	0.219 ± 0.006 (12)	16.3	90.3 ± 0.1	3.0658 (8)	12.529 (5)	3.8694 (10)
LP77	0.173 ± 0.005 (10)	15.2	77.1 ± 0.6	3.0633 (8)	12.539 (5)	3.8664 (10)
LP42	0.162 ± 0.008 (12)	25.8	42.5 ± 0.7	3.0680 (2)	12.527 (1)	3.8699 (2)

[a] Average.
[b] Two standard deviations of the mean.
[c] Number of measurements.

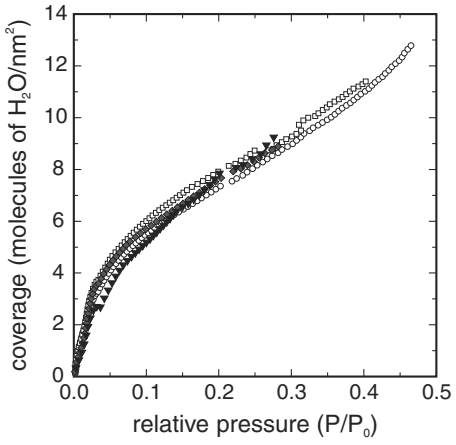

Fig. 1. Coverage of the surfaces of lepidocrocite samples as a function of relative water pressure (P/P_0). LP42—▼, LP77—◆, LP90—□, LP103—○. Small jumps of the data for sample LP42 around $P/P_0 = 0.03$ and for the sample LP90 at $P/P_0 = 0.32$ are likely instrumental artifact rather than a sample property.

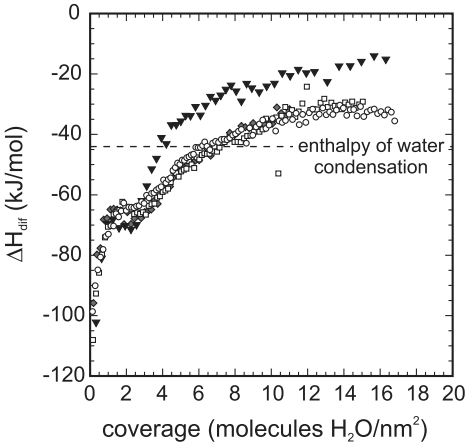

Fig. 2. Differential heat of water adsorption on lepidocrocite samples as function of H_2O coverage of the surface. Symbols: LP42—▼, LP77—◆, LP90—□, LP103—○.

Approximately at this pressure, the differential heat of adsorption reached the value for bulk water condensation of −44 kJ/mol (Fig. 2). Calorimetric results of water adsorption experiments shown on Figs. 2 and 3 were plotted as function of surface coverage θ in H_2O molecules/$nm^2$of surface, which was calculated as follows:

$$\theta_j = \frac{\sum_{1}^{j} w_i \cdot 4.46 \cdot 10^{-5} \cdot m \cdot N_A}{SA} \quad (7)$$

where N_A—Avogadro's number and SA is the total surface area of sample in nm^2. The quantity of adsorbed water was first corrected for the adsorption on the sample holder walls and then the coverage was calculated again. For the finer samples, this correction did not exceed 11% because the sample adsorbed a significant amount of water. The coarsest sample is the one most sensitive to this correction. In this case, 30% of the total adsorbed water was that adsorbed on the walls of the sample vessel. Thus, the calorimetric and water coverage data for the coarsest sample LP42 have a larger experimental uncertainty than for the finer samples.

The coverage at which the differential enthalpy of water adsorption reaches the energetics of bulk water

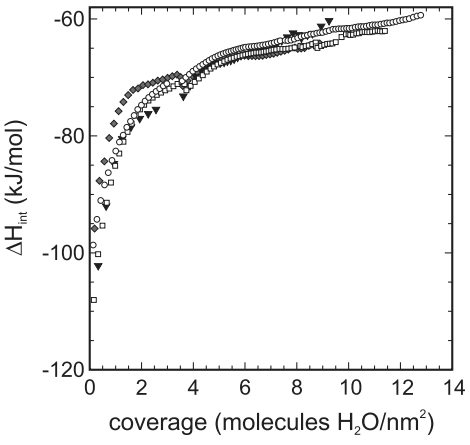

Fig. 3. Integral heat of water adsorption on lepidocrocite samples as function of H_2O coverage of the surface. Integral heat of adsorption as well as coverage was corrected for the amount of water adsorbed on the sample holder. LP42—▼, LP77—◆, LP90—□, LP103—○. Small jumps at coverages ~4–5 H_2O/nm^2 are due to the water corrections. They results from the uneven data distribution and do not indicate experimental problem.

condensation is $\theta = 6.2 \pm 0.3$ H_2O/nm^2 (average of the coverages of the samples LP103, LP90, and LP77). We will call all water adsorbed up to $\theta = 6.2$ H_2O/nm^2 chemisorbed water and the water adsorbed after that amount

physisorbed water. We emphasize that such division is based purely on our calorimetric results and not on any knowledge of the structure of the adsorbed water film. The coverage of $\theta = 6.2$ H_2O/nm^2 (i.e., only chemisorbed water on the surface) corresponds to 41.3% of all water adsorbed on the surfaces of the finer samples (LP90, LP77, LP103) at 22–25 °C and relative humidity (RH) of 43–53%. Under the same conditions, the coarser sample (LP42) adsorbs only 23% (at coverage ~6.1 H_2O/nm^2) of the water as chemisorbed water. We specify this temperature and RH for an easy comparison and experimental reproducibility among various iron oxides because these conditions are continuously maintained in the laboratory. The total water content and therefore the percentage of physically and chemically bound water will be different at other value of RH.

The integral enthalpies of water adsorption at the coverage $\theta = 6.2 \pm 0.3$ H_2O/nm^2 are comparable for all samples (see Table 2) and average to a value of -65.8 ± 2.6 kJ/mol of water. This value was used to correct the acid-solution calorimetric data for the chemisorbed water assuming $\Delta H_{desorption} = -\Delta H_{adsorption}$.

The results of acid-solution calorimetry are shown in Table 3 and plotted as a function of surface area in Fig. 4. Using a thermochemical cycle outlined in Table 4, we calculated the enthalpy of formation (ΔH_f^o) using the sample LP42 as a reference phase.

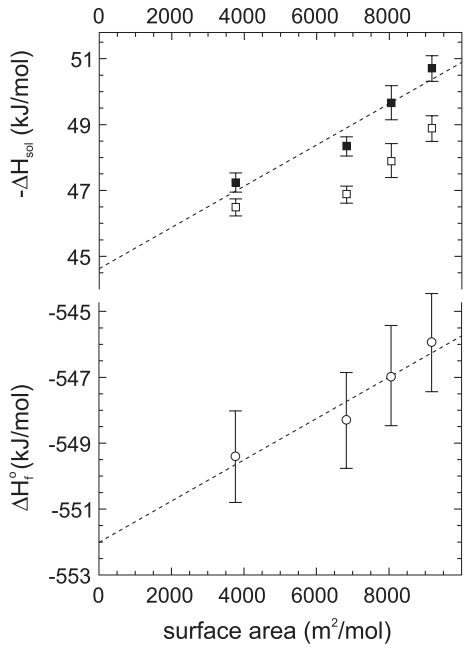

Fig. 4. Enthalpies of the studied lepidocrocite samples as a function of their surface area; upper panel: measured enthalpy of solution in 5 N HCl—□ (ΔH_1, see Tables 3 and 4), enthalpy of solution in 5 N HCl corrected for the adsorbed water—■ (ΔH_4, see Tables 3 and 4); lower panel: enthalpy of formation at standard temperature and pressure from the elements—○ (ΔH_7, see Tables 3 and 4). The slope of the linear fits through the ■ data points is equal to the surface enthalpy of anhydrous (0.62 ± 0.14 J/m^2) surface of lepidocrocite.

Table 2
Results of water adsorption calorimetry

Sample	Coverage at liquid water level, H_2O/nm^2	Integral ΔH_{ads} kJ/mol of H_2O at liquid water level	Amount of chemisorbed water % of total	
			c[a], mol	Adsorbed water[b]
LP103	5.84	−65.0	0.089	37.1
LP90	6.43	−65.8	0.086	39.4
LP77	6.27	−66.3	0.071	41.3
LP42	6.10	−66.0	0.038	23.7
Average	6.2 ± 0.3	-65.8 ± 2.6		

[a] The values of c were calculated based on the assumption that the water adsorbed between coverages of 0–6.2 H_2O/nm^2 is chemisorbed, and the water adsorbed at coverage larger than 6.2 H_2O/nm^2 is physisorbed.
[b] At 22 °C and fixed relative humidity.

Table 3
Acid-solution calorimetric data

Sample	$\Delta H_1 = \Delta H_{sln}$	$\Delta H_4 = \Delta H_{sln,corr}$	$\Delta H_7 = \Delta H_f^o$
LP103	-48.9[a] ± 0.4[b] (4)[c]	−50.7	-545.9 ± 1.5
LP90	-47.9 ± 0.5 (6)	−49.7	-547.0 ± 1.5
LP77	-46.9 ± 0.3 (6)	−48.4	-548.3 ± 1.5
LP42	-46.5 ± 0.3 (5)	−47.2	-549.4 ± 1.4

The reactions 1, 4, and 7 whose enthalpy changes are given in this table are defined in Table 4. All values are in kJ/mol.
[a] Average.
[b] Two standard deviations of the mean.
[c] Number of measurements.

Table 4
Thermochemical cycle for the calculation of the formation enthalpy of lepidocrocite samples

Reaction number and reaction	
1	$FeOOH{\cdot}xH_2O$ (cr) + $[3H^+] = [Fe^{3+} + (0.5+x)H_2O]$
2	H_2O (physisorbed = liquid) = H_2O (chemisorbed, c)
3	H_2O (liquid) = $[H_2O]$
4	FeOOH (cr) + $[3H^+] = [Fe^{3+} + 0.5H_2O]$
4A	FeOOH(sample LP42) (cr) + $[3H^+] = [Fe^{3+} + 0.5H_2O]$
5	FeOOH(sample LP42) (cr) = FeOOH (cr)
6	Fe (cr) + O_2 (g) + 0.5H_2 (g) = FeOOH(sample LP42) (cr)
7	Fe (cr) + O_2 (g) + 0.5H_2 (g) = FeOOH (cr)

Abbreviations: (cr), crystalline; (l), liquid. Species given in square brackets are in the acidic aqueous solution.
ΔH_1 = enthalpy of dissolution the lepidocrocite samples in 5 N HCl, experimental data (see Table 3).
ΔH_2 = enthalpy of adsorption of the chemisorbed water relative to physisorbed (bulk liquid) water = $-65.8 - (-44.0) = -21.8 \pm 2.6$ kJ/mol.
ΔH_3 = enthalpy of dilution of 5 N HCl solution (Parker, 1965) = −0.54 kJ/mol.
$\Delta H_4 = \Delta H_1 + c\Delta H_2 - x\Delta H_3$ = enthalpy of dissolution of a lepidocrocite sample with dry surface in 5 N HCl.
ΔH_{4A} = enthalpy of dissolution of the sample LP42 with dry surface in 5 N HCl.
$\Delta H_5 = \Delta H_{4A} - \Delta H_4$ = enthalpy of the samples relative to the coarse-grained lepidocrocite sample (LP42).
ΔH_6 = enthalpy of formation of the coarse-grained lepidocrocite from elements at 25 °C = -549.4 ± 1.4 (Majzlan et al., 2003).
$\Delta H_7 = \Delta H_6 + (\Delta H_{4A} - \Delta H_4)$ = enthalpy of formation of the lepidocrocite samples from coarse-grained hematite and liquid water at 298.15 K.

Values for the ΔH_f^o and ΔH_{sol} are given in the Table 3. The enthalpy of solution for a hypothetical lepidocrocite with zero surface area was calculated as the intercept (equal to -44.6 ± 0.6 kJ/mol) of the linear fit through the enthalpies of solution corrected for the water adsorption (Fig. 4, symbols ■). Using this value and calorimetric cycle in Table 4, the enthalpy of formation of hypothetical sample of lepidocrocite was calculated and is equal to -552.0 ± 1.6 kJ/mol. Surface enthalpies were calculated from the slopes of the best linear fit through the calorimetric data plotted versus surface area. We took into account uncertainties for each data point, and used reduced chi-criteria to evaluate deviation of sample from a theoretical distribution (Zar, 1999). The obtained values for the enthalpy of a relaxed (hydrated) and anhydrous surface are 0.40 ± 0.16 J/m^2 and 0.62 ± 0.14 J/m^2, respectively.

4. Discussion

All samples show similar behavior in coverage versus integral enthalpy of water adsorption (Fig. 2) as well as a reproducible plateau at coverages starting from $\theta \sim 1.2$ and ending at $\theta \sim 3.0$ H_2O/nm^2 with the differential enthalpy equal to -66 ± 3 kJ/mol (-76 ± 2 kJ/mol for the integral enthalpy). Such a plateau was not observed in water adsorption experiments performed in our laboratory with other iron oxides (Mazeina et al., 2006) and in water adsorption experiments with other oxides such as Al_2O_3 (Castro et al., 2006), or HfO_2 (Ushakov and Navrotsky, 2005). However, the reproducibility of the plateau and its presence in the scans for all lepidocrocite samples excludes an experimental error as its cause. We can also exclude the incorporation of water into the interlayer space as a cause for this plateau. The difference of lattice parameter *b* (equal to the interlayer spacing in lepidocrocite) for the samples with dry surfaces and those soaked in water is only 0.02–0.04 Å. If water was incorporated in the interlayer space, this difference would be significantly larger. Therefore, the water molecules are only adsorbed on the surface during our adsorption experiments and do not enter the interlayer space.

Very often, such steps or plateaus are not observed (Champion and Halsey, 1953) due to non-uniform and cooperative adsorption (Halsey, 1948). On a plane uniform surface, adsorption would proceed in a stepwise fashion as pressure increases (Champion and Halsey, 1953). A plateau observed during the hydration of the lepidocrocite surface might mean that this phase possesses such plane(s). Additionally, adsorption on this plane should be non-cooperative, that is, the adsorption of water molecules at a surface site will not modify the adsorption energy at a neighboring site. Non-cooperative adsorption can also take place if the neighboring sites are too far apart and act as isolated, non-interacting sites.

An atomistic understanding of the water adsorption on the surface of lepidocrocite would require the use of detailed spectroscopy and/or molecular modeling, be it molecular dynamics simulation or *ab initio* calculations. Only then the reasons for the existence of the plateau could be sought. Our data provide only a bulk view of the adsorption process and therefore provide little direct molecular insight into the process. Thus we may only speculate about the cause for the plateau (see Fig. 2) in the measured adsorption enthalpy. It is possible that after the initial hydration up to $\theta \sim 1.2$ H_2O/nm^2, the surface relaxes and the differential enthalpy of water adsorption to relatively abundant sites directly on the surface remains constant until higher coverage ($\theta \sim 3.0$ H_2O/nm^2) is reached. Afterwards, the differential enthalpy continues to decrease in magnitude to the level of enthalpy of water condensation (Fig. 2).

Surface enthalpy of a phase is defined as the enthalpy necessary to create a unit area of surface. By this definition, surface enthalpy refers to a surface with no adsorbed molecules, be they water or any other adsorbent. Our acid-solution calorimetric measurements, however, had to be performed on samples with hydrated surfaces. Having measured the enthalpy of water adsorption, we were able to account for the effect of water adsorption on the surface enthalpy of lepidocrocite (see calculations in Table 4). Doing so, we calculated the surface enthalpy of lepidocrocite as 0.62 ± 0.14 J/m^2 as a slope of the linear fit of corrected calorimetric data (see Table 3) plotted versus surface area. Because surfaces of minerals in soils and loose sediments are always hydrated, the enthalpy of a hydrated, relaxed surface is of equal, if not greater, interest, for geochemical and mineralogical applications. The thermodynamic properties of such a surface can be calculated from our data. By converting all chemisorbed water to physisorbed water (reaction 2 in Table 3), we create a relaxed surface covered by a thin film of H_2O that behaves in a thermodynamic sense like liquid water. Because this water has no excess energy of interaction with the surface, we may consider and treat such sample as a mechanical mixture of lepidocrocite and water. After accounting for the water in the thermochemical cycle (see Table 4), the enthalpy of lepidocrocite samples with relaxed surfaces remain. The thermodynamic properties for each lepidocrocite samples are then calculated in this way and a linear fit through the data points (enthalpy versus surface area) gives the enthalpy of the relaxed surface of 0.40 ± 0.16 J/m^2.

The lepidocrocite particles are dominated by the {0 1 0} pinacoids (Miller indices according to the orientation of symmetry elements in the space group $Cmc2_1$) (Cornell and Schwertmann, 2000). The dominance of this form allows one to neglect all other forms when considering the surface structure of the particles. In addition, this form represents the growth as well as the cleavage planes. If the layered structure of lepidocrocite is cleaved along (0 1 0), it is very likely that only the weak hydrogen bonds operating between the layers will be broken (Fig. 5). Such a surface is both charge-neutral and requires destruction of the weakest bonds in the plane of the surface. It therefore fullfils the two conditions of the most probable surface created

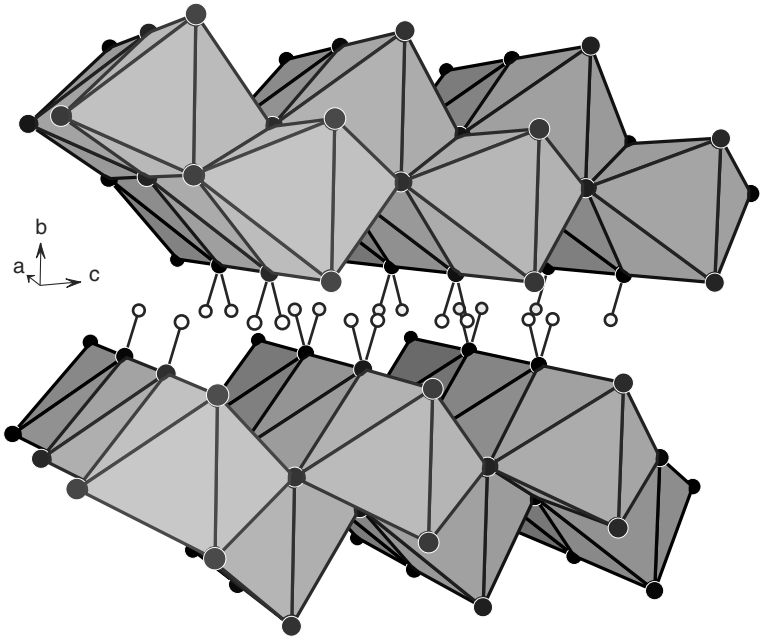

Fig. 5. Octahedral layers in the structure of lepidocrocite, bound only by hydrogen bonds. Hydrogen atoms are shown by small circles. The occupancy of these positions is 0.5.

(Koretsky et al., 1998). Using this surface, the number of adsorption sites per nm^2 can be calculated. Koretsky et al. (1998) proposed five methods for such a calculation, and their results for goethite and hematite are compared to our data for lepidocrocite in Table 5. The number of surface sites for lepidocrocite was counted by the five methods of Koretsky et al. (1998). The number of surface sites can be calculated by several methods assuming this number (1) to be equal to the number of ionic or covalent bonds which had to be broken to create a surface (method 1), (2) to be equal to the number of coordinatively unsaturated atoms at the surface (method 2), (3) to be equal to the number of atoms within 1.4 Å of the highest plane of atoms in a given surface (method 3), (4) to be equal to the number of oxygens within 1.4 Å of the highest plane of atoms in a given surface (method 4), and (5) to be equal to the number of coordinatively unsaturated atoms at the surface (method 5). A coordinatively unsaturated atom is an atom at a surface with a bond valence smaller than its bond valence in the bulk structure. The bond valence decrease must be at least 0.5 in order to count that atom as a surface site. Koretsky et al. (1998) concluded that none of the methods is clearly superior, although method 1 seemed to be in the best agreement with scattered experimental data. However, we should note that method 1 always gives a value of 0 sites/nm^2 for layered structures where the layers are connected only by hydrogen or van der Waals bonds. Therefore, the method 1 cannot be used for the (0 1 0) face of lepidocrocite. Methods 2, 3, and 4 give a value of 8.4 sites/nm^2 which appears to be a realistic estimate of the number of adsorption sites at the (0 1 0) surface of lepidocrocite.

Table 5
Calculated number of sites/nm^2 for the surfaces of lepidocrocite (this study, indexed in space group $Cmc2_1$), goethite (indexed in space group *Pnma*), and hematite (Koretsky et al., 1998)

Phase	Face	Method 1	Method 2	Method 3	Method 4	Method 5[a]
Lepidocrocite	(0 1 0)	0	8.4	8.4	8.4	0
Goethite	(0 1 0)	17.4	13.1	17.4	8.7	8.7
Hematite	(0 0 1)	27.3	18.2	18.2	13.6	4.5

[a] For the calculation for method 5, the bond distances for lepidocrocite were calculated from a structural model of Zhukhlistov (2001). The bond valence values were calculated from the fitting parameters given by Brown (2002).

The number of adsorption sites (~8.4 sites/nm^2) compares roughly to the coverage at which the bulk water condensation level is reached (6.2 molecules/nm^2). The similarity of these values indicates that only the first monolayer of water adsorbs strongly, as the chemisorbed water. In terms of its thermodynamic properties, H_2O in excess of the first monolayer is simply liquid water. The weak adsorption of water may be directly related to the weakness of the bonds that have to be broken in order to form a surface on a lepidocrocite particle. Only hydrogen bonds have to be broken to expose the (0 1 0) surface of lepidocrocite and these bonds are the weakest ones in the structure of this phase. The low value of surface enthalpy of lepidocrocite, when compared to that of goethite (0.60 ± 0.10 J/m^2 for the hydrous surface, Mazeina and Navrotsky, 2005), may be due not only to the weakness of the broken hydrogen bonds, but also to the markedly lower number of adsorption sites at the surface of lepidocrocite (Table 5). This hypothesis is supported by the observations that only ~40% of the total adsorbed water on the lepidocrocite surface is chemisorbed, whereas goethite chemisorbs about

~60% of its total water and the rest is physisorbed according to the data obtained in our laboratory.

Comparison with other iron oxide phases as well as the relationship of different phases in the Fe_2O_3–H_2O system will be given in a separate paper. However, we can say now with confidence that surface energy is a variable of substantial significance in systems that comprise very small particles (nanoparticles). When considering thermodynamic properties of iron oxides in environment, a conclusive statement about their stability cannot be made without specifying the particle size of individual phases. We believe that the differences in surface energy of the invididual FeOOH polymorphs are large enough to cause energy crossovers analogous to those in the system Al_2O_3 (McHale et al., 1997). The measurements and quantification of the surface energies of all FeOOH phases is in progress and an evaluation of their stability as a function of their surface area will be published later.

5. Conclusions

For the first time, we measured the surface enthalpy and the enthalpy of water adsorption on lepidocrocite, γ-FeOOH. The surface enthalpy of a dry surface of lepidocrocite is 0.62 ± 0.14 J/m^2. By adsorbing water, the surface relaxes and its enthalpy reduces to 0.40 ± 0.16 J/m^2. The standard enthalpy of formation from elements for lepidocrocite with nominal composition FeOOH and zero surface area is -552.0 ± 1.6 kJ/mol. Water adsorption experiments showed that ~40% of total excess water is relatively strongly bound with an integral enthalpy of adsorption approximately −65 kJ/mol relative to water vapor. The remaining water is weakly adsorbed with enthalpy of adsorption of −44 kJ/mol (relative to vapor). The calculated number of adsorption sites of 8.4/nm^2 compares roughly to the coverage at which the bulk water condensation level (in terms of enthalpy) is reached (6.2 molecules/nm^2). Therefore, only the first monolayer of water adsorbs strongly. This conclusion is in agreement with the spectroscopic studies of mineral–water interfaces, for example, that of calcite (Fenter et al., 2000a) or orthoclase (Fenter et al., 2000b).

Acknowledgments

We thank two anonymous reviewers for their constructive criticism and D. Sverjensky for editorial handling of the manuscript. We are grateful to S. Ushakov for the help with water adsorption experiments. This work was supported by the U.S. Department of Energy (Grant DE-FG03-S7ER14749).

Associate editor: Dimitri A. Sverjensky

References

Barton, T.F., Price, T., Dillard, J.G., 1990. The production of γ-FeOOH in the presence of EDTA. *J. Colloid Interface Sci.* **138**, 122–127.

Boily, J.-F., Szanyi, J., Felmy, A.R., 2006. A combined FTIR and TPD study on the bulk and surface dehydroxylation and decarbonation of synthetic goethite. *Geochim. Cosmochim. Acta* **70**, 3613–3624.

Brown, I.D., 2002. *The Chemical Bond in Inorganic Chemistry*. IUCr Monograph on Crystallography 12. Oxford Science Publications, 278 pp.

Brunauer, S., Emmett, P.H., Teller, E., 1938. Adsorption of gases in multimolecular layers. *J. Am. Chem. Soc.* **60**, 309–319.

Champion, W.M., Halsey, G.D., 1953. Physical adsorption on uniform surfaces. *J. Phys. Chem.* **57**, 646–648.

Carlson, L., Schwertmann, U., 1990. The effect of CO_2 and oxidation rate on the formation of goethite versus lepidocrocite from an Fe(II) system at pH 6 and 7. *Clay Miner.* **25**, 65–71.

Castro, R., Ushakov, S.V., Gengembre, L., Gouvea, D., Navrotsky, A., 2006. Surface energy and thermodynamic stability of γ-alumina: effect of dopants and water. *Chem. Mater.* **18**, 1867–1872.

Cornell, R.M., Schwertmann, U., 2000. *The Iron Oxides*. Wiley-VCH.

Dos Anjos, L.H.C., Franzmeier, D.P., Schulze, D.G., 1995. Formation of soils with plinthite on a toposequence in Maranhao state, Brazil. *Geoderma* **64**, 257–279.

Fenter, P., Geissbühler, P., DiMasi, E., Srajer, G., Sorensen, L.B., Sturchio, N.C., 2000a. Surface speciation of calcite observed in situ by high-resolution X-ray reflectivity. *Geochim. Cosmochim. Acta* **64**, 1221–1228.

Fenter, P., Teng, H., Geissbühler, P., Hanchar, J.M., Nagy, K.L., Sturchio, N.C., 2000b. Atomic scale structure of the orthoclase (001)-water interface measured with high-resolution X-ray reflectivity. *Geochim. Cosmochim. Acta* **64**, 3663–3673.

Fitzpatrick, R.W., Taylor, R.M., Schwertmann, U., Childs, C.W., 1985. Occurrence and properties of lepidocrocite in some soils of New Zealand, South Africa and Australia. *Aust. J. Soil Res.* **23**, 543–567.

Goldman, N.T., Bender Koch, C., Singer, A., 2002. Lepidocrocite in hydrothermal sediments of the Altantis II and Thetis deeps, Red Sea. *Clay. Clay Miner.* **50**, 186–197.

Halsey, G., 1948. Physical adsorption on non-uniform surfaces. *J. Chem. Phys.* **16**, 931–937.

Koretsky, C.M., Sverjensky, D.A., Sahai, N., 1998. A model of surface site types on oxide and silicate minerals based on crystal chemistry: implications for site types and densities, multi-site adsorption, surface infrared spectroscopy, and dissolution kinetics. *Am. J. Sci.* **298**, 349–438.

Larson, A.C., von Dreele, R.B., 1994. *GSAS. General Structure Analysis System.* LANSCE, MS-H805, Los Alamos, New Mexico.

Lewis, D.G., Farmer, V.C., 1986. Infrared absorption of surface hydroxyl groups and lattice vibrations in lepidocrocite (γ-FeOOH) and boehmite (γ-AlOOH). *Clay Miner.* **21**, 93–100.

Majzlan, J., Grevel, K.-D., Navrotsky, A., 2003. Thermodynamics of iron oxides: part II. Enthalpies of formation and relative stability of goethite (α-FeOOH), lepidocrocite (γ-FeOOH), and maghemite (γ-Fe_2O_3). *Am. Miner.* **88**, 855–859.

Mazeina, L., Navrotsky, A., 2005. Surface enthalpy of goethite. *Clay. Clay Miner.* **53**, 113–122.

Mazeina, L., Deore, S., Navrotsky, A., 2006. Energetics of bulk and nano-akaganeite, β-FeOOH: enthalpy of formation, surface enthalpy and enthalpy of water adsorption. *Chem. Mater.* **18**, 1830–1838.

McHale, J.M., Auroux, A., Perrotta, A.J., Navrotsky, A., 1997. Surface energies and thermodynamic phase stability in nanocrystalline aluminas. *Science* **277**, 788–791.

Naono, H., Nakai, K., 1989. Thermal decomposition of γ-FeOOH fine particles. *J. Colloid Interface Sci.* **128**, 146–156.

Navrotsky, A., 2004. Energetic clues to pathways to biomineralization: precursors, clusters, and nanoparticles. *Proc. Nat. Acad. Sci. USA* **101**, 12096–12101.

Parker, V.B., 1965. Thermal properties of uni-univalent electrolytes. *National Standard Reference Data Series, National Bureau of Standards* 2, 66 pp.

Pitcher, M.W., Ushakov, S.V., Navrotsky, A., Woodfield, B.F., Li, G., Boerio-Goates, J., Tissue, B.M., 2005. Energy crossovers in nanocrystalline zirconia. *J. Am. Ceram. Soc.* **88**, 160–167.

Posey-Dowty, J., Moskowitz, B., Crerar, D., Hargraves, R., Tanenbaum, L., Dowty, E., 1986. Iron oxide and hydroxide precipitation from ferrous solutions and its relevance to Martian surface mineralogy. *Icarus* **66**, 105–116.

Ranade, M.R., Navrotsky, A., Zhang, H.Z., Banfield, J.F., Elder, S.H., Zaban, A., Borse, P.H., Kulkarni, S.K., Doran, G.S., Whitfield, H.J., 2002. Energetics of nanocrystalline TiO_2. *Proc. Nat. Acad. Sci. USA* **99**, 6476–6481.

Schwertmann, U., Cornell, R.M., 2000. *Iron Oxides in the Laboratory*. Wiley-VCH.

Schwertmann, U., Fechter, H., 1994. The formation of green rust and its transformation to lepidocrocite. *Clay Miner.* **29**, 87–92.

Sudakar, C., Subbanna, G.N., Kutty, T.R.N., 2003. Effect of anions on the phase stability of γ-FeOOH nanoparticles and the magnetic properties of gamma-ferric oxide derived from lepidocrocite. *J. Phys. Chem. Solids* **64**, 2337–2349.

Tagirov, B.R., Diakonov, I.I., Devina, O.A., Zotov, A.V., 2000. Standard ferric–ferrous potential and stability of $FeCl_2^+$ to 90 °C. Thermodynamic properties of $Fe(aq)^{3+}$ and ferric–chloride species. *Chem. Geol.* **162**, 193–219.

Taylor, R.M., 1984. Influence of chloride on the formation of iron oxides from iron(II) chloride. II. Effect of $[Cl^-]$ on the formation of lepidocrocite and its crystallinity. *Clay. Clay Miner.* **32**, 175–180.

Ushakov, S.V., Navrotsky, A., 2005. Direct measurements of water adsorption enthalpy on hafnia and zirconia. *Appl. Phys. Lett.* **87**, 164103/1–164103/3.

Zar, J.H., 1999. *Biostatistical analysis*. Prentice-Hall, Inc, Englewood Cliffs, NY.

Zhukhlistov, A.P., 2001. Crystal structure of lepidocrocite FeO(OH) from electron diffraction data. *Kristallografiya* **46**, 805–808.